# A very low current scanning tunneling microscope

David Dunlap, Steve Smith, Carlos Bustamante, Javier Tamayo, and Ricardo García

Citation: Rev. Sci. Instrum. **66**, 4876 (1995); doi: 10.1063/1.1146168
View online: http://dx.doi.org/10.1063/1.1146168
View Table of Contents: http://rsi.aip.org/resource/1/RSINAK/v66/i10
Published by the American Institute of Physics.

# A very low current scanning tunneling microscope

David Dunlap
*DIBIT III A3, Istituto Scientifico San Raffaele, 20132 Milano, Italy*

Steve Smith and Carlos Bustamante
*Institute of Molecular Biology, University of Oregon, Eugene, Oregon 97403*

Javier Tamayo and Ricardo García[a)]
*Centro Nacional de Microelectronica, CSIC, Serrano 144, 28006 Madrid, Spain*

(Received 28 November 1994; accepted for publication 10 July 1995)

The applications of the scanning tunneling microscope (STM) in air are usually restricted to good conducting materials as clean metals, doped and passivated semiconductors, or to some molecular adsorbates deposited onto graphite. In order to study poor conducting materials as biological molecules, we have built a very low current STM. This instrument can routinely be operated at 0.1 pA while having a bandwidth of 7 kHz. The advantages of using very low currents are illustrated by imaging 5-nm-thick purple membranes. These membranes can only be imaged at currents smaller than 2 pA. © *1995 American Institute of Physics.*

## I. INTRODUCTION

The scanning tunneling microscope (STM) has become a powerful instrument for structural analysis[1] of surfaces and atomic or nanometer-scale modification of metallic, semimetallic, and semiconducting materials.[2] The physical parameter measured in scanning tunneling microscopy is an electron current flowing between a sharp metallic tip and the sample. In standard conditions the STM is operated at about 1 nA. This implies that the sample under study has to sustain current densities of about $10^6$ A/cm$^2$. Partially oxidized metallic and semiconducting surfaces and biological molecules deposited on conducting substrates are difficult to study with a STM operated at standard currents (about 1 nA) due to their poor electrical conductivity, or equivalently the high gap resistance of the tip–sample interface.

Although high resolution, topographic images of poorly conducting and insulating surfaces can be obtained by scanning force microscopy,[3,4] scanning tunneling microscopy of these samples is still desirable because the STM can also be used to probe the electronic properties of these surfaces. One approach to imaging poorly conducting materials with the STM involves the operation of a combined force and tunneling microscope.[5–7] Another strategy to overcome the problems associated with poorly conducting materials is to operate a STM at very low currents and relatively high voltages.[8–11]

In this second approach, instrumental features limit the extent to which the current may be decreased in scanning tunneling microscopy. The minimum detectable current depends on the thermal noise across the resistors of the current-to-voltage ($I$-$V$) converter. For a constant temperature $T$, and resistance $R$, the root mean square noise in the feedback voltage signal $V$ increases with the square root of the bandwidth of the feedback[12] $\Delta f$. Thus very small currents may be detected if the bandwidth is decreased.

$$V_{\mathrm{rms}} = \sqrt{4kTR\Delta f}, \tag{1}$$

where $k$ is Boltzmann's constant. However, maintaining an adequately broad bandwidth in the feedback system is desirable in STM, because the bandwidth limits the speed of image acquisition. The scan speed multiplied by the highest spatial frequency in the area to be imaged yields the highest frequency input signal which must fall within the bandwidth of the feedback. The largest gain stage in the feedback loop is typically the high gain, $I$-$V$ converter, and therefore the current amplifier constraints the bandwidth of the feedback. If the bandwidth of the amplifier is too narrow (the response is too slow), the feedback system will not be sufficiently responsive and the tip will not faithfully track the surface. The simple relationship $v_t = \Delta f / X$ between the scan speed (tip velocity) $v_t$, the amplifier bandwidth $\Delta f$, and the highest spatial frequency component in the image $X$, defines an upper limit for the scan speed. A spatial frequency of 10 cycles/nm at 7 kHz bandwidth establishes a maximum scan speed of 700 nm/s. Rapid image acquisition is often very important in scanning tunneling microscopy, among other advantages, it minimizes the distortions introduced by low frequency mechanical instabilities and thermal drift.

A very low current STM (it will be called picoampere STM hereafter) is described below. It operates at currents as low as 0.07 pA, yet it has a sufficiently broad bandwidth, to record a 512×512 point image in several minutes. The picoampere STM is controlled by the electronics and software of a commercially available scanning probe microscope. In performance tests, the instrument recorded atomic features on highly oriented pyrolytic graphite (HOPG) and imaged biological molecules that cannot support high current densities. The utility of imaging with subpicoampere tunneling currents is highlighted in studies of purple membrane. This membrane, at relatively high voltages, can only be imaged at currents smaller than 2 pA.

## II. INSTRUMENT

A standard STM has three major elements: the tip–sample stage, the electronic control unit that transmits analog voltage data from the current-to-voltage converter to the

a)Author to whom correspondence should be addressed.

 0034-6748/95/66(10)/4876/4/$6.00 

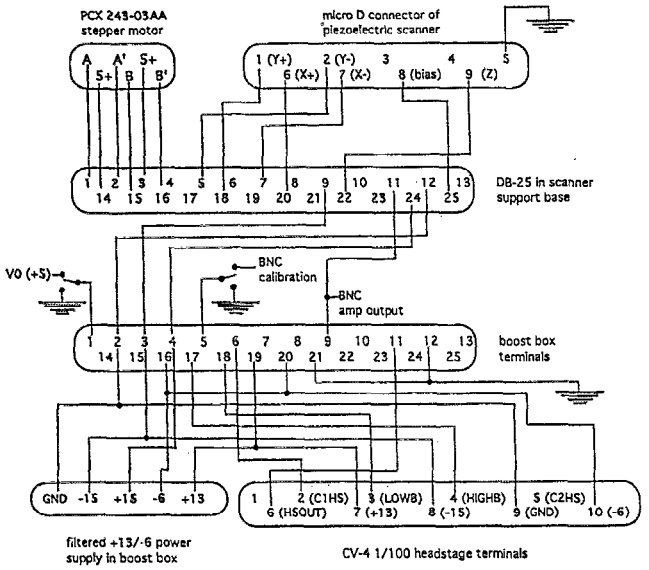


FIG. 1. A diagram of the wiring between the components of the low current STM illustrates the connections required to utilize the CV-4 1/100 patch clamp amplifier in the scanned sample configuration.

computer and digital control parameters from the computer to the piezoelectric positioners in the tip–sample stage, and the control and display software. Software and control units are available from a number of manufacturers. What follows is a description of a low current STM that utilizes a patch clamp amplifier integrated into the electronics and control software of the Nanoscope II-III scanning probe microscope (Digital Instruments, Santa Barbara, CA). It might also be adapted to software and electronics from other sources.

The low current STM requires two custom components: a probe housing which contains the tip holder and carries the low current amplifier electronics, and the scanner support base which houses electrical connections and the stepper motor for automated approach of the tip to the sample surface.

The amplifier is a key factor for achieving simultaneously very low currents and wide bandwidth feedback response. The picoampere STM was constructed utilizing the CV-4 1/100 amplifier (Axon Instruments, Foster City, CA). This is a selectable (low/high) gain amplifier developed for patch clamp experiments. The amplifier consists of a headstage with the electrical probe input and the $I$-$V$ converter, and a "boost box" that houses circuitry to tune the frequency response of the amplifier and select the gain. On the high gain setting, currents less than 1 pA can be measured while maintaining a bandwidth of 7 kHz. The headstage electronics are housed in a small metal box. One end of the box has a 1.3-mm-diam metal, female plug in a teflon collar where the electrical probe is inserted. Bundled copper wires at the other end of the box connect the headstage to the boost box. A DB-9 pin coupling was spliced into this wiring, so that the headstage/probe housing could be easily removed for access to the sample stage of the scanner.

For use as a patch clamp amplifier, the boost box is connected via a DB-25 pin plug to the controlling electronics. For the present use, those connections and some circuitry were modified (Fig. 1) to provide the appropriate power and control signals from the Nanoscope electronics. The boost box and headstage (amplifier) are powered by the $\pm 15$ V sources available on the 25 pin ribbon cable to the scanner support base. A low noise power supply installed in the boost box generates $+13$ and $-6$ V sources for the headstage from the $\pm 15$ V sources. Control signals are toggled by two switches installed on the boost box. One switch is used to select either high or low gain. The other switch selects either the normal operating mode or the frequency response calibration mode using a signal input through a BNC connector installed on the boost box. A second BNC installed in the boost box carries the amplifier output signal for use in calibration.

The front side of the probe housing has a hinged aluminum frame electrically connected with an inset indium tin oxide coated glass window. The bottom is a steel plate that articulates with the three magnetic adjustment screws of the scanner. This surface must have a kinematic mount consisting of a conical groove and a conical pit positioned around a large central opening. The headstage of the amplifier is mounted on top of the probe housing, secured by a flat aluminum strap, such that the teflon collar protrudes slightly into the internal cavity along the central axis of the probe housing. In this way the thermal expansion of the housing surrounding the probe is bilaterally symmetric to minimize thermal drift.

The tip holder consists of a flat metal strip and small tweezers that hold the tip. The flat side is attached to a teflon cylinder that has two small magnets. This cylinder is screwed to the top of the probe housing and forms a female coupling which mates with the teflon collar of the headstage. A small metal wire joins the support of the tip holder and the amplifier (Fig. 2).

The support base that cradles the piezoelectric scanner is a hollow aluminum cylinder capped by a thick aluminum plate on the upper end. Inside there is a stepper motor (PCX 243-03AA, Vexta, Oriental Motor Corporation, Japan) to automatically lower the tip to the sample surface. Electrical connections are also routed through the base. On top of the aluminum plate, a scanner support ring is mounted on four posts cut from plastic tubing.

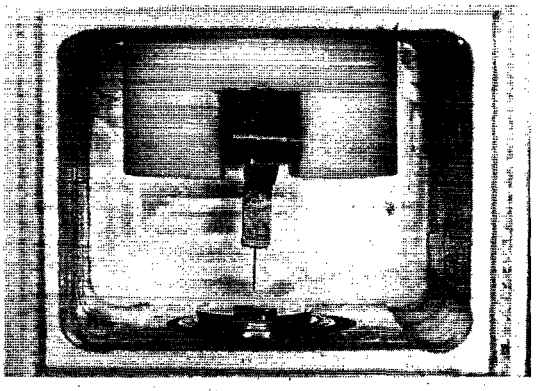

FIG. 2. In this configuration of the low current STM, the tip remains stationary and the sample is scanned in a raster pattern by the piezoelectric tube upon which it rests.

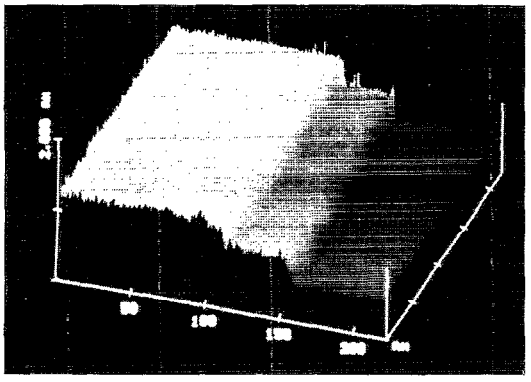

(a)

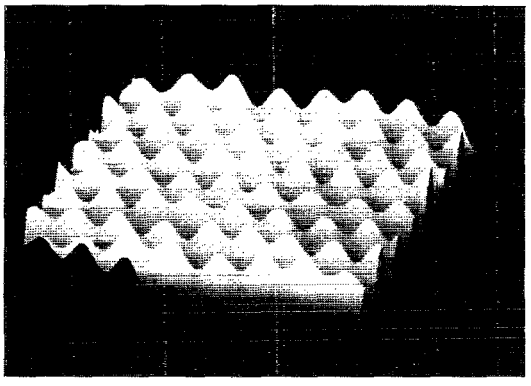

(b)

FIG. 3. STM image of a HOPG surface. (a) Several terraces separated by monoatomic steps are observed in this scan recorded at 1 pA and 41 mV; scan size, 221 nm×221 nm. (b) The atomic structure of the HOPG surface in a small region of a terrace viewed at 70 pA and 5 mV; scan size 2.1 nm×2.1 nm.

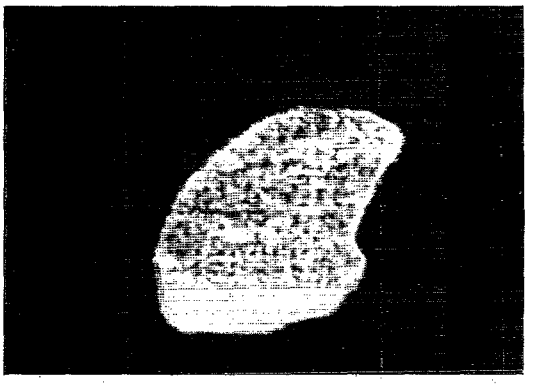

(a)

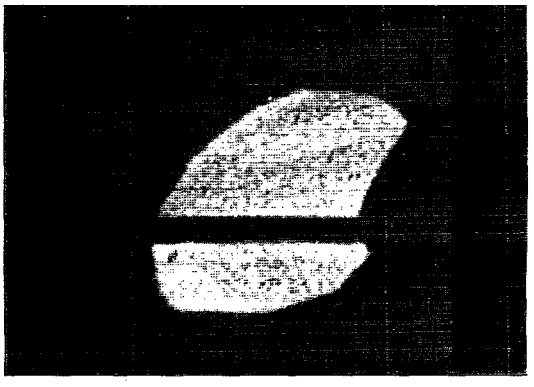

(b)

FIG. 4. Topographic images of purple membrane adsorbed to HOPG (1.47 $\mu$m×1.47 $\mu$m. (a) The image was recorded at 0.2 pA and −7.6 V (electrons emitted from the sample). (b) A horizontal band of protein was stripped from the middle of the membrane by scanning at 20 pA and −7.6 V, and could be seen when the whole membrane was imaged at 0.20 pA and −7.6 V afterwards.

The amplifier was calibrated for a dc input and separately tuned to optimize the frequency response. A variable voltage from a potentiometer connected to a 9 V battery was applied to a 2 GΩ resistor that was connected to the tip holder. The applied voltage and the amplifier output were displayed simultaneously on an oscilloscope and the dc gain was adjusted with a gain potentiometer in the boost box. To optimize the frequency response of the amplifier, a triangular voltage waveform was applied, through a capacitor present in the headstage circuitry, to the input of the amplifier. The calibration signal was input through a BNC installed on the boost box that was connected to this capacitor via terminal 5 of the boost box. Since the current across a capacitor is proportional to the derivative of the voltage across the capacitor, $i=C(dV/dt)$, the current cycles between positive and negative values at the frequency of the triangular wave. The amplifier response was observed on an oscilloscope and tuned using a series of seven potentiometers in the boost box to achieve the squarest response possible. The dc gain measured 50 mV/pA with the high gain selected ($R=50$ GΩ). With this calibration in effect, images were recorded at currents as low as 0.07 pA. At room temperature and for a bandwidth of 7 kHz the thermal noise of the amplifier is calculated to be 0.05 pA ($I=V_{\rm rms}/R$).

## III. EXPERIMENT

The performance of the STM was tested by imaging a well-defined surface such as HOPG. This surface exhibits large, atomically flat terraces separated by monoatomic steps [Fig. 3(a)]. On the terraces, the hexagonal lattice of carbon atoms can be seen [Fig. 3(b)].

A technologically as well as biologically interesting object was imaged to illustrate one of the potential applications of a very low current STM. Purple membrane (PM) is a natural membrane crystal made of a single protein species, bacteriorhodopsin.[13] Previously Guckenberger *et al.* have shown that low currents are required to image purple membranes.[14] The proteins are packed into a hexagonally symmetric lattice with a constant of 6.3 nm.[15] The membranes typically appear in oval sheets of about 1 $\mu$m in diameter and 4.8 nm in thickness. Purple membranes have been proposed as components in prototypes of some optical devices.[16]

A 10 $\mu$l drop of an aqueous suspension containing 0.1 mg/ml of PM was sprayed onto a piece of freshly cleaved graphite (HOPG). Without any further preparation the sample was placed in the STM chamber for imaging.

The experiment consists of imaging the membrane at several currents and comparing the differences. Figure 4(a)

shows a PM sheet imaged at a tunneling current of 0.2 pA and a bias voltage of −7.6 V. Although at the scale of the image no details of the protein packing are revealed, the membrane sheet is clearly resolved against the substrate. Subsequently, a horizontal band of the central membrane was scanned at 20 pA. Then the whole membrane was imaged again at 0.2 pA [Fig. 4(b)]. This second, low current image reveals a substrate level band which bisects the membrane that corresponds to the region scanned at 20 pA. Apparently the overlying proteins were removed by the tip. Similar results have been obtained scanning other regions of the membrane at 3 pA. Furthermore, these observations have been reproduced with all the membrane sheets under study. These results suggest that for a fixed voltage the membrane behaves as an effective resistor $R_{\text{eff}}$. When the current is set to a value that implies an interface resistance smaller than $R_{\text{eff}}$, the STM extends the tip toward the membrane. The approach of the tip toward the surface produces mechanical contact. Such contact displaces the adsorbed protein layer as the tip scans laterally.

Poor conductivity through the purple membrane might be attributed to low electron mobility or to the small number of available states for transport, or both. The precise physical process responsible for this behavior is not completely established yet.[10]

These experiments show that noncontact imaging of purple membrane at relatively high voltages can only be achieved below 2 pA of tunneling current. Such small currents imply that STM images can be formed by averaging about 1000 electrons for each data point, which is three orders of magnitude less than for standard STM currents. The picoampere STM described above has sufficiently broad bandwidth to record such images within several minutes. This capability enabled routine imaging of a biological specimen. This work and other recent work (Guckenberger *et al.*[11]) suggest that high voltage and low current constitute the basis for a scanning tunneling microscopy mode that is generally applicable for investigating structural biology.

## ACKNOWLEDGMENTS

We would like to thank T. Del Val and J. A. Vela for technical assistance. R.G. has received financial support from the Direccion General Investigación Científica y Técnica DGICYT (Spain) under Contract No. PB94-0016.

[1] *Scanning Tunneling Microscopy and Related Methods*, edited by R. Behm, N. García, and H. Rohrer (Kluwer Academic, Dordrecht, 1990), NATO ASI Series, Series E: Applied Sciences, Vol. 184.
[2] *Atomic and Nanometer-Scale Modification of Materials: Fundamentals and Applications*, edited by P. Avouris (Kluwer Academic, Dordrecht, 1993), NATO ASI Series, Series E: Applied Science, Vol. 239
[3] G. Binnig, C. Quate, and C. Gerber, Phys. Rev. Lett. **56**, 930 (1986).
[4] D. Rugar and Paul Hansma, Physics Today, October, 23 (1990).
[5] M. Specht, F. Ohnesorge, and W. Heckl, Surf. Sci. Lett. **257**, L653 (1991).
[6] M. Salmeron, A. Folch, G. Neubauer, W. Kolbe, D. F. Ogletree, and M. Tomitori, Ultramicroscopy **41-42** 1113 (1992).
[7] D. Anselmatti, C. Gerber, B. Michel, H.-J. Güntherodt, and H. Rohrer, Rev. Sci. Instrum. **63**, 3003 (1992).
[8] R. Guckenberger, W. Wiegräbe, A. Hillerbrand, T. Hartmann, Z. Wang, and W. Baumeister, Ultramicroscopy **31**, 327 (1989).
[9] R. García, Appl. Phys. Lett. **64**, 1162 (1994).
[10] R. García, J. Tamayo, J. M. Soler, and C. Bustamante, Langmuir **11**, 2109 (1995).
[11] R. Guckenberger, M. Heim, G. Cevc, H. Knapp, W. Wiegräbe, and A. Hillerbrand, Science **266**, 1538 (1994).
[12] C. Kittel and H. Kroemer, *Thermal Physics* (W. H. Freeman, New York, 1980).
[13] D. Osterhelt and W. Stoeckenius, Nature New Biology **233**, 149 (1971).
[14] R. Guckenberger, B. Hacker, T. Hartmann, T. Scheybani, Z. Wang, W. Wiegräbe, and W. Baumeister, J. Vac. Sci. Technol. B **9**, 1227 (1991).
[15] R. Henderson, J. M. Baldwin, T. A. Ceska, F. Zemlin, E. Beckman, and K. H. Downing, J. Mol. Biol. **213**, 899 (1990).
[16] R. Birge, in *Nanotechnology*, edited by B. C. Crandall and J. Lewis (MIT Press, Cambridge, 1992).